# INTERACTION OF VORTEX BREAKDOWN WITH A FLEXIBLE FIN AND ITS CONTROL, PHASE-3.

**Final Report**

**submitted to**

**Dr. Charbel N Raffoul**
**Chief of Aeronautical Sciences**
**European Office of Aerospace Research & Development (EOARD)**
**223/231 Old Marylebone Road**
**NW1 5TH London, UK**

**by**

**Dr. Ismet Gursul**
**Department of Mechanical Engineering**
**University of Bath**
**Bath, BA2 7AY**
**United Kingdom**

**October 24, 2001**

# REPORT DOCUMENTATION PAGE

Form Approved OMB No. 0704-0188



| 1. REPORT DATE *(DD-MM-YYYY)* | 2. REPORT TYPE | 3. DATES COVERED *(From – To)* |
|---|---|---|
| 24 10 2001 | Final Report | 10/26/00 - 26-Oct-01 |

**4. TITLE AND SUBTITLE**

Interaction of Vortex Breakdown with a Flexible Fin and its Control, Phase-3

**5a. CONTRACT NUMBER**
F61775-01-WE006

**5b. GRANT NUMBER**

**5c. PROGRAM ELEMENT NUMBER**

**6. AUTHOR(S)**

Dr. Ismet Gursul

**5d. PROJECT NUMBER**

**5d. TASK NUMBER**

**5e. WORK UNIT NUMBER**

**7. PERFORMING ORGANIZATION NAME(S) AND ADDRESS(ES)**
University of Bath
Claverton Down
Bath BA2 7AY
United Kingdom

**8. PERFORMING ORGANIZATION REPORT NUMBER**
N/A

**9. SPONSORING/MONITORING AGENCY NAME(S) AND ADDRESS(ES)**

EOARD
PSC 802 BOX 14
FPO 09499-0014

**10. SPONSOR/MONITOR'S ACRONYM(S)**

**11. SPONSOR/MONITOR'S REPORT NUMBER(S)**
SPC 01-4006

**12. DISTRIBUTION/AVAILABILITY STATEMENT**

Approved for public release; distribution is unlimited.

**13. SUPPLEMENTARY NOTES**

**14. ABSTRACT**

This report results from a contract tasking University of Bath as follows: The proposed research is the third (and last) phase for a comprehensive study on the interaction of vortex breakdown with a flexible fin. The study is to conclude with a summary on the techniques that would control or reduce these interactions. The first two phases were supported by AFOSR. In the first phase, the effect of fin deflections on vortex breakdown was investigated. In the second phase, the interaction with vortex breakdown, by using a flexible fin was developed. In this phase, alternative control techniques applied on or around the fin, such as 1) Application of suction on the fin; 2) Blowing jet at the trailing edge of the fin; 3) Use of synthetic jet at the trailing edge will be investigated. Initial experiments will be performed in the water tunnel for the sake of flow visualization. Additional experiments in the 2.12m x 1.51m low-speed wind tunnel will be performed to demonstrate the applicability of the proposed control methods at higher Reynolds numbers. The results will also serve as a verification tool for the on-going numerical simulations performed at AFRL/VA.

**15. SUBJECT TERMS**
EOARD, Aero-Structure Interface, Vortex flows, Fin Buffeting

| 16. SECURITY CLASSIFICATION OF: | | | 17. LIMITATION OF ABSTRACT | 18, NUMBER OF PAGES | 19a. NAME OF RESPONSIBLE PERSON |
|---|---|---|---|---|---|
| a. REPORT | b. ABSTRACT | c. THIS PAGE | | | Charbel N. Raffoul |
| UNCLAS | UNCLAS | UNCLAS | UL | 28 | 19b. TELEPHONE NUMBER *(Include area code)* +44 (0)20 7514 4299 |

## ABSTRACT

Several flow control methods were explored to control fin buffeting. These include suction around the fin, trailing-edge jet, and synthetic jet as documented in previous progress reports. From these, only the trailing-edge jet offered significant potential and was studied in detail. Effect of a trailing-edge jet on the interaction of a leading-edge vortex with a fin and resulting fin buffeting was investigated in water tunnel as well as wind tunnel experiments. Flow visualization showed that fin-induced vortex breakdown can be delayed into the wake even for the head-on collision of the leading-edge vortex with the fin. Hence it was demonstrated that the adverse pressure gradient due to the presence of the fin could be overcome with a deflected trailing-edge jet. Delay of vortex breakdown into the wake even for relatively small values of jet velocity ratio is possible for deflected jets, whereas the effectiveness of the jet with no deflection is very limited. Buffeting response of a flexible fin in wind tunnel experiments showed that there was considerable delay of the onset of buffeting to higher angles of attack with increasing jet momentum for $\beta=30°$ and 45°. Depending on the fin location with respect to the leading-edge vortex, it was possible to shift the buffeting envelope as much as 12° in incidence of the wing. Wind tunnel experiments also showed that the nozzle geometry is very important and causes very different buffeting envelopes for the same momentum coefficient.


## INTRODUCTION

Experimental evidence suggests that several unsteady flow phenomena may cause fin buffeting. These phenomena and their physical models were recently discussed by Gursul and Xie[1]. However, vortex breakdown phenomenon is the most important source of buffeting over delta wings. A wide variety of investigations were conducted on both simplified fin-delta wing configurations and fins on actual model aircraft in order to understand the mechanisms of fin buffeting and the relation to the vortical flow fields over the wing[2-13]. A good summary of the experimental investigations is given by Wolfe[8] et al.

Both structural control and flow control methods have been used by previous investigators to attenuate fin buffeting. Structural methods include increasing the

stiffness and damping. There have also been attempts to reduce the buffeting with active vibration control techniques using piezoelectric actuators[14] or an active rudder[15], without any knowledge of the flow field. Unfortunately, only modest reductions in fin response are possible with the structural control methods in the absence of any flow control method. Regarding flow control methods, several techniques are available in order to alter the position of the vortex with respect to the fin, or delay vortex breakdown. These include blowing[16] and suction[17] on the wing surface, fences[3], and variable position leading-edge extensions[18]. Common to these investigations was the introduction of modifications well upstream of the breakdown and close to the origin of the vortex. However, these methods are not effective over a wide range of angle of attack encountered during a maneuver because of drastic changes in the position of the vortex. Moreover, the effectiveness of these techniques reaches a saturation with increasing control parameter (such as the blowing coefficient) as one tries to delay the location of vortex breakdown, because vortex breakdown phenomenon strongly depends on the external pressure gradient. Trailing-edge of the wing, and more importantly, the fin itself produce and adverse pressure gradient, which is the dominant factor in determining the location of vortex breakdown and the magnitude of fin buffeting. Limited effectiveness of the above mentioned flow control techniques is due to incapability of altering the external pressure gradient while modifying the structure of the vortices.

The purpose of this study is to investigate a different aspect of vortex control technique, which is more likely to alter the external pressure gradient, and involves a jet at the trailing-edge of the wing. As the beneficial effects of trailing-edge blowing on vortex breakdown over delta wings are well known[19-22], this has a good potential to overcome the adverse pressure gradient due to the trailing-edge and the fin, and to delay vortex breakdown and attenuate fin buffeting. Thrust vectoring remains as a preferred method of integrating propulsive and lift systems for modern fighter aircraft, which can have thrust/weight ratio larger than unity[23]. This means that large amount of mass injection through trailing-edge jets is possible. This study concentrates on the effects of a trailing-edge jet on fin buffeting.

## EXPERIMENTAL SETUP

### Water tunnel experiments

Initial experiments with trailing-edge blowing were performed in a water tunnel because of its advantages in flow visualization. The water tunnel has a horizontal working section, with a cross-sectional area of 15 inches by 20 inches. The delta wing and fin were designed and scaled to those used in the wind tunnel experiments previously reported elsewhere[24]. The wing and rigid fin are shown in Figure 1. The chord length is c=250 mm, giving a Reynolds number around Re=25,000 for $U_\infty$=10 cm/sec. At the maximum angle of attack $\alpha$=40°, the blockage ratio was 6%, and no correction on the data was attempted. The fin was attached to the trailing-edge of the wing with a screw, and the location of the fin could be varied from $y_f/s$=0.0 to 1.0 with increments of 0.1.

For the trailing-edge blowing experiments, a rectangular nozzle with an aspect ratio of 6 and a width of 30 mm was placed underneath the wing as shown in Figure 1. The centerline of the nozzle coincided with the approximate position of the vortex axis ($y/s \approx 0.6$) within the range of angle of attack tested. (The spanwise location of the vortex was estimated from the pressure measurements across the span at x/c=0.5 in the absence of the fin[24]. It was found that the location of the suction peak is only slightly affected by the angle of attack, showing that the spanwise location of the leading edge vortex is roughly constant). An important parameter was jet deflection angle $\beta$, which was generated by using a thin plate to deflect the jet (see Figure 1). The volumetric flow rate of the jet was measured by a rotameter, which was placed at the discharge side of a submersible pump as shown in Figure 2. The maximum jet velocity obtained was $U_{jet}/U_\infty$=8.9, which corresponds to a momentum coefficient of

$$C_\mu = \rho U_{jet}^2 A_{jet} / \frac{1}{2} \rho U_\infty^2 S_w = 0.708.$$

As the thrust/weight ratio can be larger than unity[23], one can show that the momentum coefficient can take up values on the order of unity. Therefore, the values of the momentum coefficient used in the experiments are realistic, and also consistent with the range used by the other investigators[19-22]. In the water tunnel experiments, dye flow visualization was used to visualize the vortex trajectories and breakdown location. A digital video camera was used to record the flow visualization and to further analyze the

results. The measurement uncertainty for vortex breakdown location was 1% of the chord length. Estimated uncertainty for the momentum coefficient was 2%.

**Wind tunnel experiments**

Additional experiments in a 2.12 m by 1.51 m low-speed wind tunnel were carried out to demonstrate the applicability of the proposed control methods at higher Reynolds numbers. A flexible fin shown in Figure 3a was designed and fabricated. It consists of a thin aluminum spar surrounded by several wood segments to provide aerodynamic shaping. The advantages that the wood sections offer are low material density and ease of fabrication. These sections were attached to the spar with small bolts. With this design, the contribution of the wood sections to the bending stiffness of the spar is minimized. The dimensions of the spar were chosen to obtain the natural frequencies of the first bending mode for a typical modern combat aircraft. The thickness of the spar was 2 mm. The leading-edge of the fin was double bevelled at an angle of 30 deg. The main dimensions of the fin are given in Figure 3a. The spar was attached to the delta wing by a bracket near the trailing-edge of the wing.

The experimental setup, which uses a half-model delta wing and a splitter plate, is shown in Figure 3b. The delta wing model had a sweep angle of $\Lambda=75°$ and a chord length of c=500 mm. The lee surface was flat, whereas the leading-edges were bevelled at 45° on the windward side. The thickness of the delta wing was 15 mm. The Reynolds number based on the chord length was $Re=3.5*10^5$. The dimensions of the delta wing and fin are scaled to those used in the water tunnel experiments. Buffeting response of this flexible fin was investigated by measuring the fin vibration levels sensed by a tip accelerometer attached to the spar. The measurement uncertainty for the tip acceleration is estimated as 2%. In addition to the calculating the rms value of the fin tip acceleration, the spectra of the tip acceleration was examined for each case. The fin vibrations occurred at the natural frequency of the first bending mode, which is little influenced by the angle of attack.

An identical nozzle scaled to one used in the water tunnel experiments was connected to pressured air supply to produce the trailing-edge jet. The mass flow of the

jet was monitored by a rotameter, and the maximum momentum coefficient obtained was $C_\mu$=0.287.

## RESULTS

### Water tunnel experiments

Previous wind tunnel investigation[24] using a flexible fin showed that the fin location $y_f/s$ is a very important parameter in addition to the angle of attack. Outboard fin locations produce very light buffeting, surprisingly even at high angle of attack. Inboard fin locations may produce the heaviest buffeting, depending on the angle of attack. At low to moderate angles of attack, the buffeting is light. An example is shown in Figure 4 (a) for $y_f/s$=0.2 and $\alpha$=25°. At high angle of attack, in particular when the shear layer impinges on the fin, the heaviest buffeting is observed. An example is shown in Figure 4 (b) for $y_f/s$=0.2 and $\alpha$=35°. A particularly interesting configuration is for $y_f/s$=0.6, which corresponds to the approximate position of the vortex axis within the range of angle of attack tested. An example is shown in Figure 4 (c) for $\alpha$=23°. Due to the adverse pressure gradient produced by the presence of the fin, vortex breakdown is always observed upstream of the fin. This head-on collision of the vortex with the fin produces moderate level of buffeting, when compared to heavy buffeting produced for inboard fin locations. Consequently, we focused on the fin locations $y_f/s$=0.2, 0.4, and 0.6 in this study.

Figures 5-7 show flow visualization pictures for (a) no flow control, and (b) jet blowing at the maximum flow rate ($U_{jet}/U_\infty$ = 8.9, $C_\mu$=0.708) for $y_f/s$=0.2, 0.4, and 0.6. The angle of attack is $\alpha$=31° and the jet deflection angle $\beta$=30°. It is seen that vortex breakdown is delayed into the wake for all three fin locations when the jet is turned on. In fact, even for the head-on collision ($y_f/s$=0.6), it is possible to eliminate the breakdown completely. Effect of the velocity ratio $U_{jet}/U_\infty$ on the location of vortex breakdown is shown in Figure 8 for $\alpha$=30° and $\alpha$=40° for various jet deflection angles $\beta$. Figure 8 (a) shows that complete elimination of vortex breakdown even for relatively small values of jet velocity ratio is possible for deflected jets, whereas the effectiveness of the jet with no deflection ($\beta$=0°) is very limited. Positive effect of jet deflection in delaying vortex

breakdown was noted previously for a delta wing[20] and with no fin. Our results for $y_f/s=0.2$ is consistent with those of Reference 20. Similar observations can be made from Figure 8 (b) for a higher angle of attack, although flow control is less effective overall. No attempts were made to study the effect of deflection angle in detail, and only four values of $\beta$ were used in the current experiments. Nevertheless, the results suggest that there may be an optimum value of $\beta$, which may depend on the angle of attack. Consequently we performed detailed flow visualization experiments for $\beta=30°$ and for $\beta=0°$ for comparison.

Figures 9 and 10 show the variation of breakdown location as a function of angle of attack for three fin locations for $\beta=0°$ and 30° respectively. In each case, no flow control ($U_{jet}/U_\infty = 0$) and jet blowing at the maximum flow rate ($U_{jet}/U_\infty = 8.9$, $C_\mu=0.708$) are compared. Each data point represents the time-averaged breakdown location, and large scatter of data is observed, in particular for the jet blowing, which indicates the unsteady character of vortex/jet interaction. It is seen in Figure 9 that, for $\beta=0°$, vortex breakdown location is delayed 20% to 30% of the chord length with a trailing-edge jet. For $\beta=30°$ shown in Figure 10, the delay is around 40% to 60% of the chord length. For $y_f/s=0.2$ and 0.4, vortex can be completely eliminated up to an angle of attack of around 35°. Even for the head-on collision case $y_f/s=0.6$, for which vortex breakdown is always upstream of the fin, breakdown can be eliminated up to $\alpha=30°$ with jet blowing. A summary of the results presented in Figures 9 and 10 is shown in Figure 11 together with the results for no fin case. It is seen that, for $U_{jet}/U_\infty = 0$, breakdown location for all three fin locations is further upstream compared to no fin case, and the effect of fin location is negligible for $x_{bd}/c \le 0.6$. For $U_{jet}/U_\infty = 8.9$ ($C_\mu=0.708$), breakdown location for $y_f/s=0.2$, 0.4, and no fin case roughly collapse, whereas vortex breakdown for the head-on collision case is further downstream.

The results presented so far show that vortex breakdown due to the presence of a fin can be completely eliminated by a trailing-edge jet even at high angle of attack. Most likely reason behind this improvement is that the trailing-edge jet creates a favorable pressure gradient near the trailing-edge[20] and reduces the adverse pressure gradient due to the fin. However, there are other factors such as entraintment effects suggested by

Reference 19 and the interaction between the jet and the wing vortices[25]. Wang et al[25] showed that wing vortices may be drawn toward the jet center by the induced velocity created by the jet vortices. Figure 12 show flow visualization pictures for (a) $U_{jet}/U_\infty = 0$, (b) $U_{jet}/U_\infty = 8.9$ (in a "steady-state case"), (c) right after the jet is turned off, for the following parameters: $y_f/s=0.2$, $\alpha=30°$, $\beta=30°$. It is seen that the leading-edge vortex is drawn toward the jet, and is nearly parallel to the jet in the steady-state case. When the jet is turned off, the wing vortex realigns itself to become nearly parallel to the free stream. Then the vortex breakdown slowly propagates upstream, and eventually reaches a steady-state location similar to that shown in Figure 12 (a). The role of jet entraintment and jet/vortex interactions deserves further studies.

**Wind tunnel experiments**

In order to quantify the effect of trailing-edge jet on the buffeting of the flexible fin, detailed experiments were carried out for $y_f/s$= 0.2, 0.4, 0.6, and jet deflection angles $\beta=0°$, 15°, 30°, and 45°. Figure 13 shows the variation of the rms tip acceleration as a function of angle of attack for various momentum coefficients, for the fin location $y_f/s=0.2$. It is seen that the effect of the jet momentum is very small for $\beta=0°$, but there is considerable delay of the onset of buffeting with increasing jet momentum for $\beta=30°$ and 45°. It is possible to shift the buffeting envelope as much as 8° in angle of attack at the largest momentum coefficient. Hence, blowing at the trailing-edge appears to be more effective at the higher jet deflection angles. These results are consistent with the flow visualization pictures obtained in the water tunnel (see Figures 8-10). Figure 14 shows the variation of the rms tip acceleration as a function of angle of attack for various $\beta$ and $y_f/s=0.4$. Again there is negligible effect for $\beta=0°$, whereas delays of as much as 12° in the buffeting onset incidence are possible at high jet deflection angles. The results for $y_f/s=0.2$ and 0.4 are very similar, with clear delays in buffeting response to higher angles of attack when the jet is turned on, although the buffeting levels are somewhat smaller for $y_f/s=0.4$.

Figure 15 shows the variation of the rms tip acceleration as a function of angle of attack for various $\beta$ and $y_f/s=0.6$. Note that, for this fin location, the spanwise position of

the vortex axis coincides with the location of the fin leading-edge. For this "head-on collision" case, vortex breakdown is always observed upstream of the fin, and the overall level of buffeting is smaller than that of $y_f/s$=0.2 and 0.4. It is seen in Figure 15 that the variation of the rms tip acceleration with angle of attack is also more gradual compared to other cases. The effect of jet blowing at the trailing-edge is very small for this fin location for all jet deflection angles tested.

Limited experiments were performed in order to study the effect of nozzle geometry. In particular, the nozzle aspect ratio and the nozzle width to wing semispan ratio may be important parameters. The dimensions, width/semispan ratio, and aspect ratio of several nozzles tested are given in Table 1. The original nozzle is denoted as case A in the table. In order to make a comparison of the effect of nozzle geometry, the momentum coefficient was kept the same for all nozzles tested. The last column in Table 1 shows the velocity ratio $U_{jet}/U_\infty$ for the maximum momentum coefficient used for the original nozzle ($C_\mu$=0.287). Figure 16 shows the variation of the rms tip acceleration as a function of angle of attack for four nozzles at various jet deflection angles for $C_\mu$=0.287 and $y_f/s$=0.4. Buffeting response differs very little for $\beta$=0° and 15°, but there are large effects of nozzle geometry for $\beta$=30° and 45°. At these large deflection angles, the original nozzle appears to be more effective in delaying the onset of buffeting, although there is an accompanying increase in the maximum levels of buffeting. Also, although the velocity ratio $U_{jet}/U_\infty$ is the smallest for the original nozzle (case A, see Table 1), it provides the best performance. In fact, there is a trend that jet blowing becomes less effective with increasing $U_{jet}/U_\infty$ for the constant $C_\mu$. Clearly there remain several aspects of the effect of nozzle geometry to be studied in future work.

| Nozzle | Dimensions | Width/semispan | Aspect ratio | $U_{jet}/U_\infty$ ($C_\mu$=0.287) |
|---|---|---|---|---|
| A | 60 x 10 mm$^2$ | 0.45 | 6 | 4 |
| B | 60 x 5 mm$^2$ | 0.45 | 12 | 5.66 |
| C | 60 x 2.5 mm$^2$ | 0.45 | 24 | 8 |
| D | 30 x 5 mm$^2$ | 0.22 | 6 | 8 |

Table 1: Dimensions, width/semispan, aspect ratio, and velocity ratio for nozzles.

## CONCLUSIONS

Effect of a trailing-edge jet on the interaction of a leading-edge vortex with a fin and resulting fin buffeting was investigated in water tunnel as well as wind tunnel experiments. Flow visualization studies showed that vortex breakdown is induced as a result of the adverse pressure gradient imposed by the fin, but can be delayed into the wake with increasing jet momentum coefficient. Even for the head-on collision of the leading-edge vortex with the fin, it was possible to eliminate the breakdown completely. Delay of vortex breakdown into the wake even for relatively small values of jet velocity ratio is possible for deflected jets, whereas the effectiveness of the jet with no deflection is very limited. For $\beta=30°$, vortex breakdown can be delayed up to 60% of the chord length depending on the fin location with respect to the leading-edge vortex. Buffeting response of a flexible fin in wind tunnel experiments showed that the effect of jet momentum was very small for $\beta=0°$, but there was considerable delay of the onset of buffeting to higher angles of attack with increasing jet momentum for $\beta=30°$ and $45°$. It was found that it was possible to shift the buffeting envelope as much as $12°$ in incidence of the wing. The wind tunnel tests showed that blowing at the trailing-edge appears to be more effective at higher jet deflection angles, which is consistent with the flow visualization results obtained in the water tunnel.

The results presented in this paper show that vortex breakdown due to the presence of a fin can be delayed by a trailing-edge jet, with resulting attenuation of fin buffeting. It is suggested that the jet creates a favorable pressure gradient and reduces the adverse pressure gradient due to the fin. However, there are several factors that need further studies: effect of jet entraintment, vortex interactions between the jet and wing vortices, and the effect of nozzle geometry. Our limited wind tunnel experiments showed that the nozzle geometry is very important and causes very different buffeting envelopes for the same momentum coefficient.

## ACKNOWLEDGMENT

This work was sponsored by the European Office of Aerospace Research and Development, Air Force Office of Scientific Research, USAF, under Contract No. F61775-01-WE006.

## REFERENCES

1. Gursul, I., and Xie, W., "Buffeting Flows over Delta Wings", *AIAA Journal,* vol. 37, no. 1, 1999, pp. 58-65.

2. Triplett, W.E., "Pressure Measurements on Twin Vertical Tails in Buffeting Flow", *Journal of Aircraft,* vol. 20, no. 11, November 1983, pp. 920-925.

3. Lee, B.H.K. and Brown, D., "Wind-Tunnel Studies of F/A-18 Tail Buffet", *Journal of Aircraft,* vol. 24, no. 1, January-February 1992, pp. 146-152.

4. Washburn, A.E., Jenkins, L.N. and Ferman, M.A., "Experimental Investigation of Vortex-Fin Interaction", AIAA 93-0050, 31st Aerospace Sciences Meeting and Exhibit, January 11-14, 1993, Reno, NV.

5. Meyn, L.A. and James, K.D., "Full Scale Wind Tunnel Studies of F/A-18 Tail Buffet", AIAA-93-3519, AIAA Applied Aerodynamics Conference, 1993.

6. Lee, B.H.K. and Tang, F.C., "Characteristics of the Surface Pressures on a F/A-18 Vertical Fin Due to Buffet", *Journal of Aircraft,* vol. 31, no. 1, January-February 1994, pp. 228-235.

7. Bean, D.E. and Wood, N.J., "Experimental Investigation of Twin-Fin Buffeting and Suppression", *Journal of Aircraft,* vol. 33, no. 4, 1996, pp. 761-767.

8. Wolfe, S., Canbazoglu, S., Lin, J.C. and Rockwell, D., "Buffeting of Fins: An Assessment of Surface Pressure Loading", *AIAA Journal,* vol. 33, no. 11, 1995, pp. 223-2234.

9. Mayori, A. and Rockwell, D., "Interaction of a Streamwise Vortex with a Thin Plate: A Source of Turbulent Buffeting", *AIAA Journal,* vol. 32, no. 10, October 1994, pp. 2022-2029.

10. Wolfe, S., Lin, J.C. and Rockwell, D., "Buffeting at the Leading-Edge of a Flat Plate Due to a Streamwise Vortex: Flow Structure and Surface Pressure Loading", *Journal of Fluids and Structures,* vol. 9, 1995, pp. 359-370.

11. Canbazoglu, S., Lin, J.C., Wolfe, S. and Rockwell, D., “Buffeting of Fins: Distortion of Incident Vortex”, *AIAA Journal,* vol. 33, no. 11, November 1995, pp. 2144-2150.

12. Gordnier, R.E. and Visbal, M.R., “Numerical Simulation of the Impingement of a Streamwise Vortex on a Plate”, AIAA-97-1781, 28th AIAA Fluid Dynamics Conference, June 29-July 2, 1997, Snowmass Village, CO.

13. Gursul, I. and Xie, W., "Interaction of Vortex Breakdown with an Oscillating Fin", *AIAA Journal*, vol. 39, no. 3, 2001, pp. 438-446.

14. Hauch, R.M., Jacobs, J.H., Dima, C., and Ravindra, K., “Reduction of Vertical Tail Buffet Response Using Active Control”, *Journal of Aircraft*, vol. 33, no. 3, May-June, 1996, pp. 617-622.

15. Breitsamter, C. and Laschka, B., “Aerodynamic Active Control for EF-2000 Fin Buffet Load Alleviation”, AIAA 2000-0656, 38th Aerospace Sciences Meeting and Exhibit, 10-13 January 2000, Reno, NV.

16. Bean, D.E., Greenwell, D.I., and Wood, N.J., “Vortex Control Technique for the Attenuation of Fin Buffet”, *Journal of Aircraft,* vol. 30, no. 6, Nov.-Dec. 1993, pp. 847-853.

17. McCormick, S. and Gursul, I., “Effect of Shear Layer Control on Leading Edge Vortices”, *Journal of Aircraft,* vol. 33, no. 6, 1996, pp. 1087-1093.

18. Gursul, I., Srinivas, S. and Batta, G., “Active Control of Vortex Breakdown over a Delta Wing”, *AIAA Journal,* vol. 33, no. 9, 1995, pp. 1743-1745.

19. Helin, H.E. and Watry, C.W., “Effects of Trailing-Edge Jet Entrainment on Delta Wing Vortices”, *AIAA Journal,* vol. 32, no. 4, April 1994, pp. 802-804.

20. Shih, C. and Ding, Z., “Trailing-Edge Jet Control of Leading-Edge Vortices of a Delta Wing”, *AIAA Journal,* vol. 34, no. 7, July 1996, pp. 1447-1457.

21. Vorobieff, P.V. and Rockwell, D.O., “Vortex Breakdown on Pitching Delta Wing: Control by Intermittent Trailing-Edge Blowing”, *AIAA Journal,* vol. 36, no. 4, April 1998, pp. 585-589.

22. Mitchell, A.M., Molton, P., Barberis, D., and Delery, J., “Control of Leading-Edge Vortex Breakdown by Trailing Edge Injection”, AIAA-99-3202, 1999.

23. Ross, H., "X-31, The First Aircraft Designed for High Angle of Attack Manoeuvring", *Symposium on Advanced Flow Management, Part A-Vortex Flow and High Angle of Attack*, NATO AVT meeting, 7-11 May 2001, Loen, Norway.

24. Lambert, C. and Gursul, I., "Buffeting of a Flexible Fin Over a Delta Wing", AIAA 2001-2426, 19th AIAA Applied Aerodynamics Conference, 11-14 June, 2001, Anaheim, CA.

25. Wang, F.Y., Proot, M.M.J., Charbonnier, J.M., and Sforza, P.M., "Near-Field Interaction of a Jet with Leading-Edge Vortices", *Journal of Aircraft*, vol. 37, no. 5, September-October, 2000, pp. 779-785.

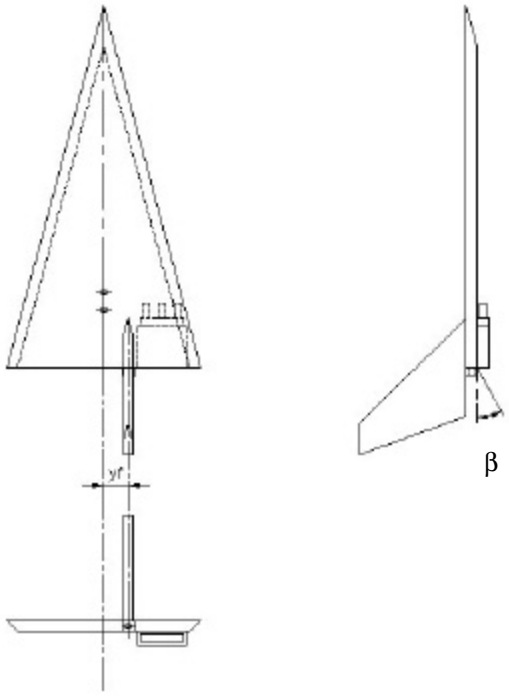


Figure 1: Definition of fin location ($y_f$) and flow deflection angle ($\beta$).

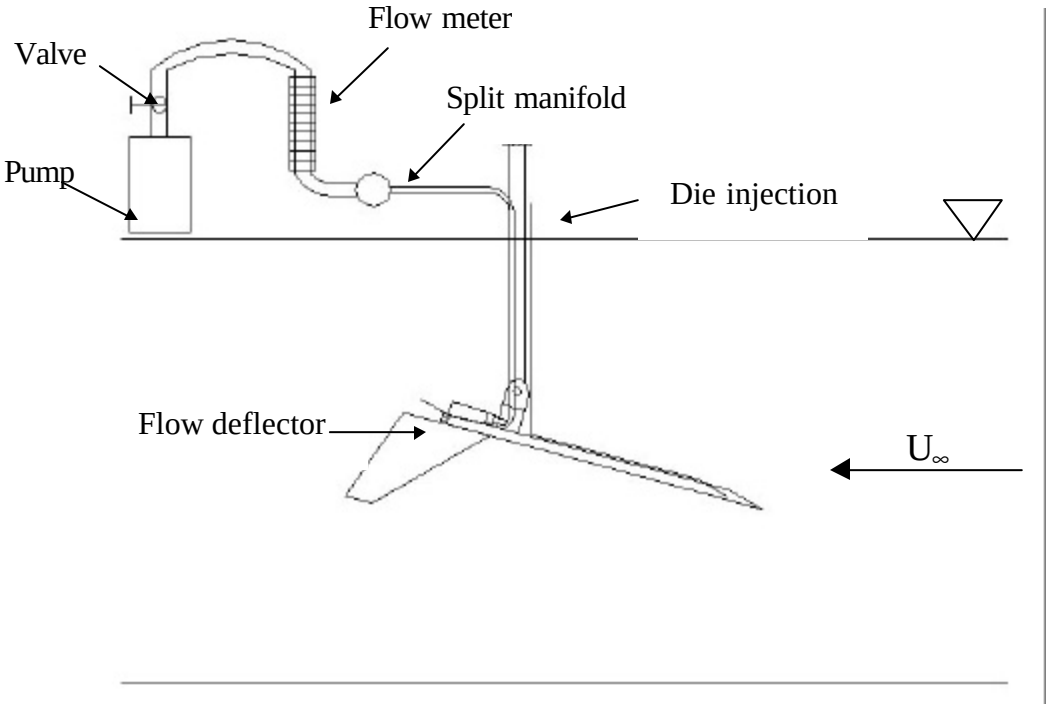


Figure 2: Schematic of the experimental set up in water tunnel.

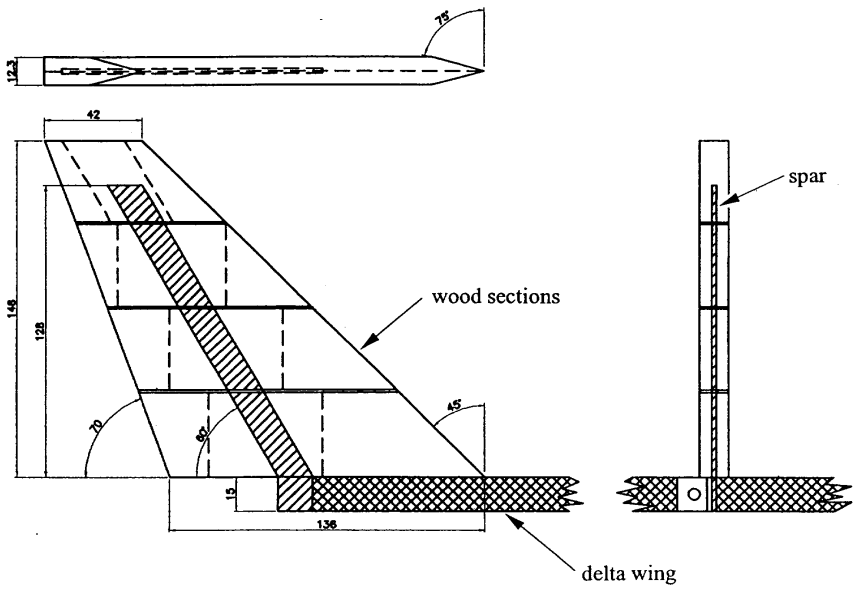


(a) Design of flexible fin.

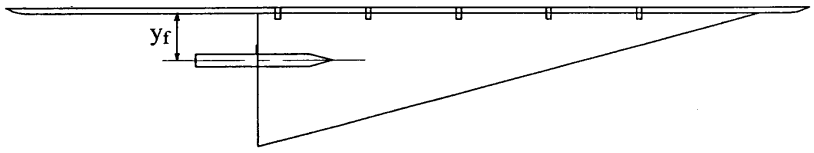


(b) Half- delta wing model, fin, and splitter plate.

Figure 3: Overview of the experimental setup in wind tunnel.

(a)

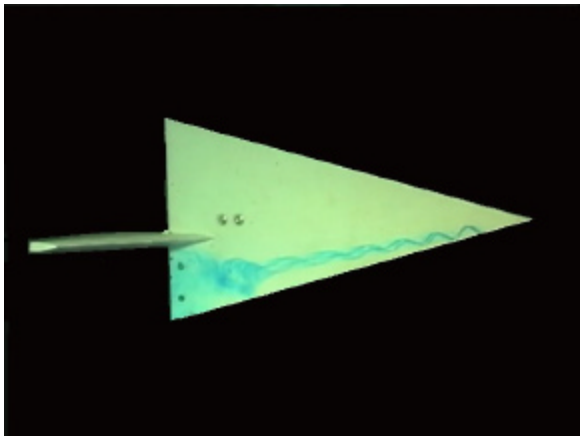

(b)

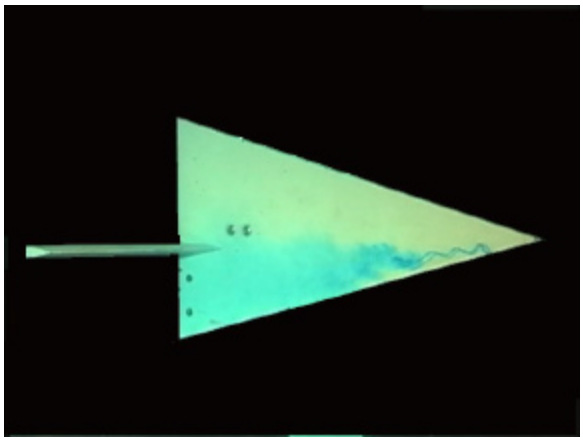

(c)

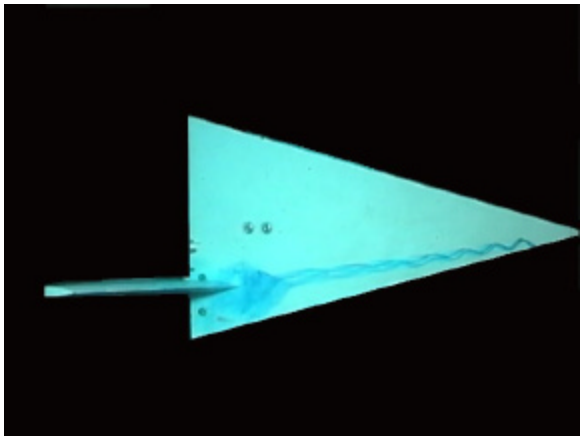

Figure 4: Flow visualization for (a) $y_f/s = 0.2$, $\alpha = 25°$, (b) $y_f/s = 0.2$, $\alpha = 35°$, (c) $y_f/s = 0.6$, $\alpha = 23°$ for no jet blowing.

(a)

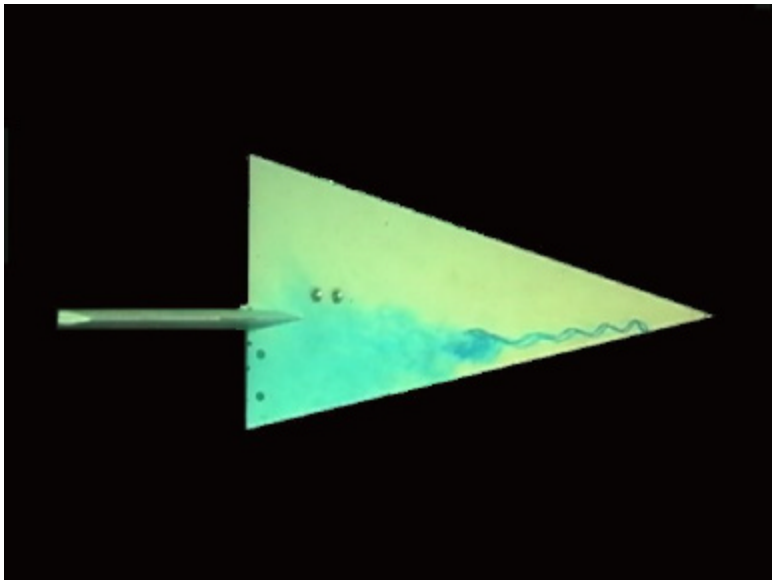

(b)

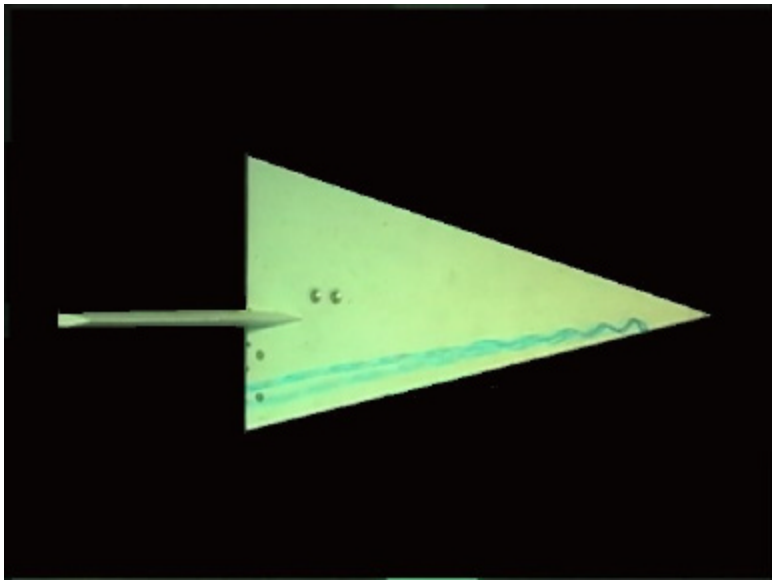

Figure 5: Flow visualization for $y_f/s = 0.2$, $\alpha = 31°$, $\beta = 30°$, (a) $U_{jet}/U_\infty = 0$ and (b) $U_{jet}/U_\infty = 8.9$ ($C_\mu$=0.708).

(a)

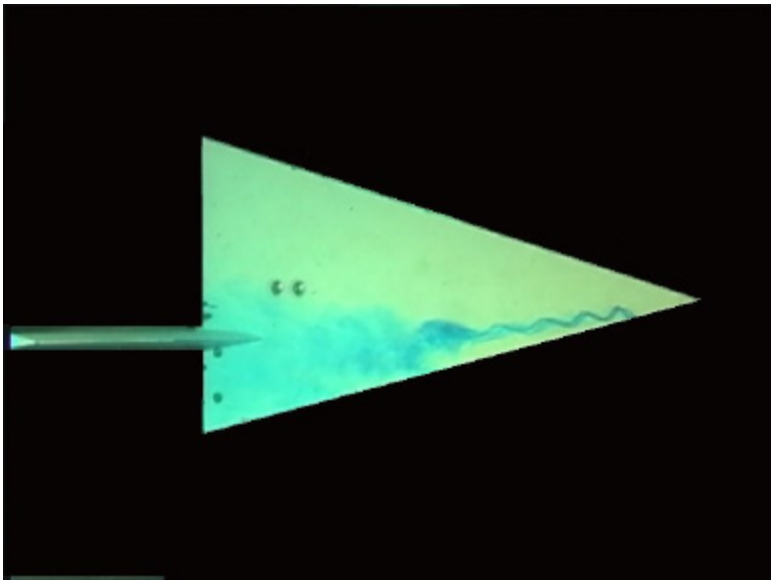

(b)

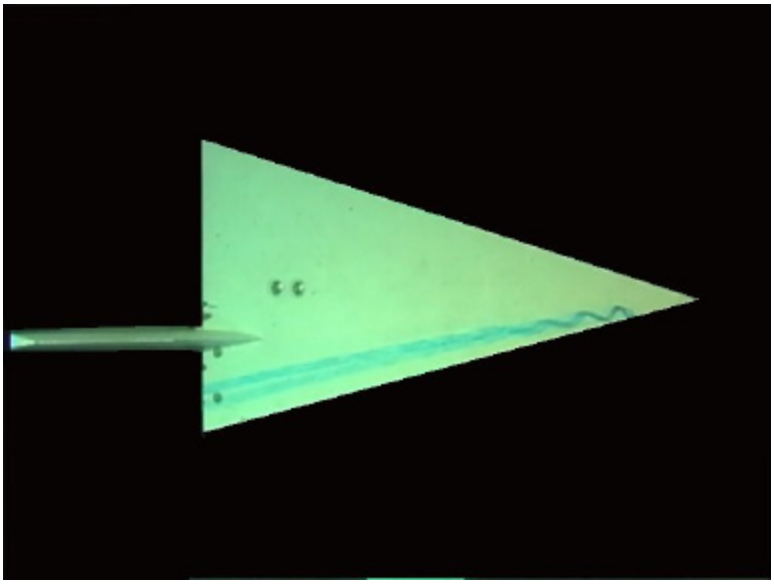

Figure 6: Flow visualization for $y_f/s = 0.4$, $\alpha = 31°$, $\beta = 30°$, (a) $U_{jet}/U_\infty = 0$ and (b) $U_{jet}/U_\infty = 8.9$ ($C_\mu$=0.708).

(a)

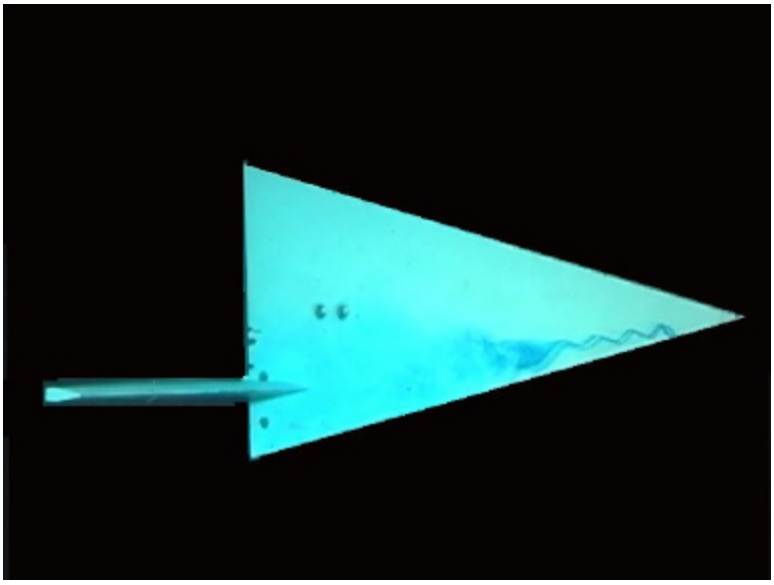

(b)

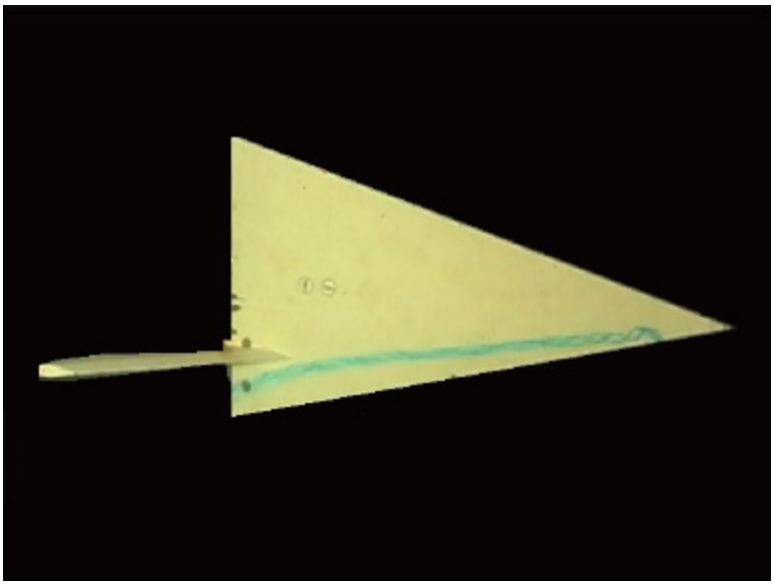

Figure 7: Flow visualization for $y_f/s = 0.6$, $\alpha = 31°$, $\beta = 30°$, (a) $U_{jet}/U_\infty = 0$ and (b) $U_{jet}/U_\infty = 8.9$ ($C_\mu$=0.708).

(a)

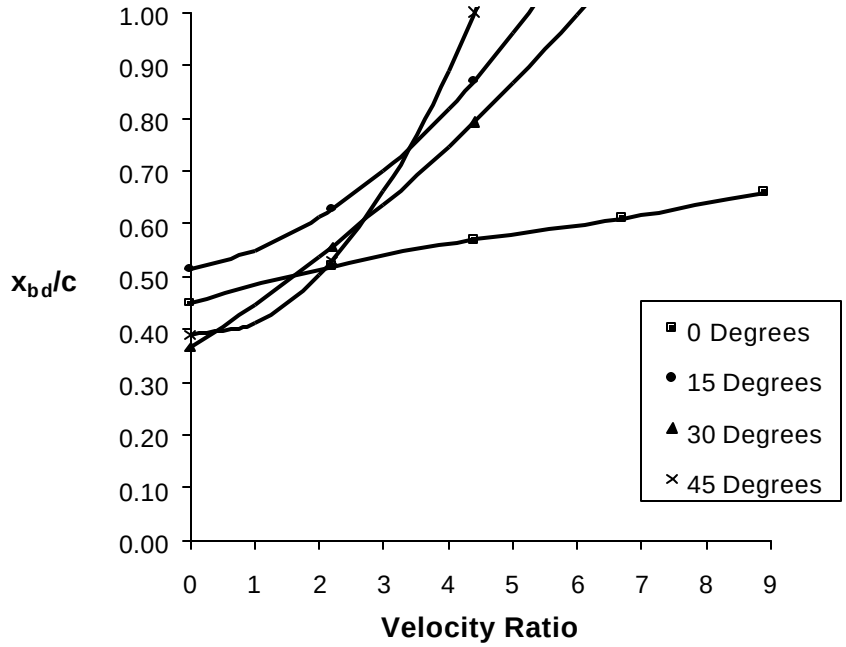


(b)

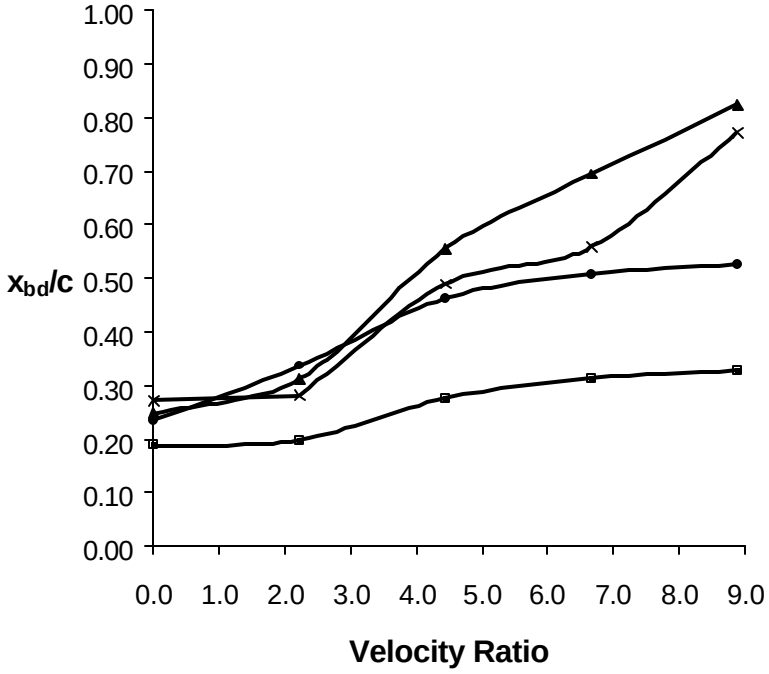


Figure 8: Variation of vortex breakdown location as a function of velocity ratio for $y_f/s$ = 0.2, jet deflection angles $\beta$ = 0°, 15°, 30° and 45°, and for (a) $\alpha$ = 30°, (b) $\alpha$ = 40°.

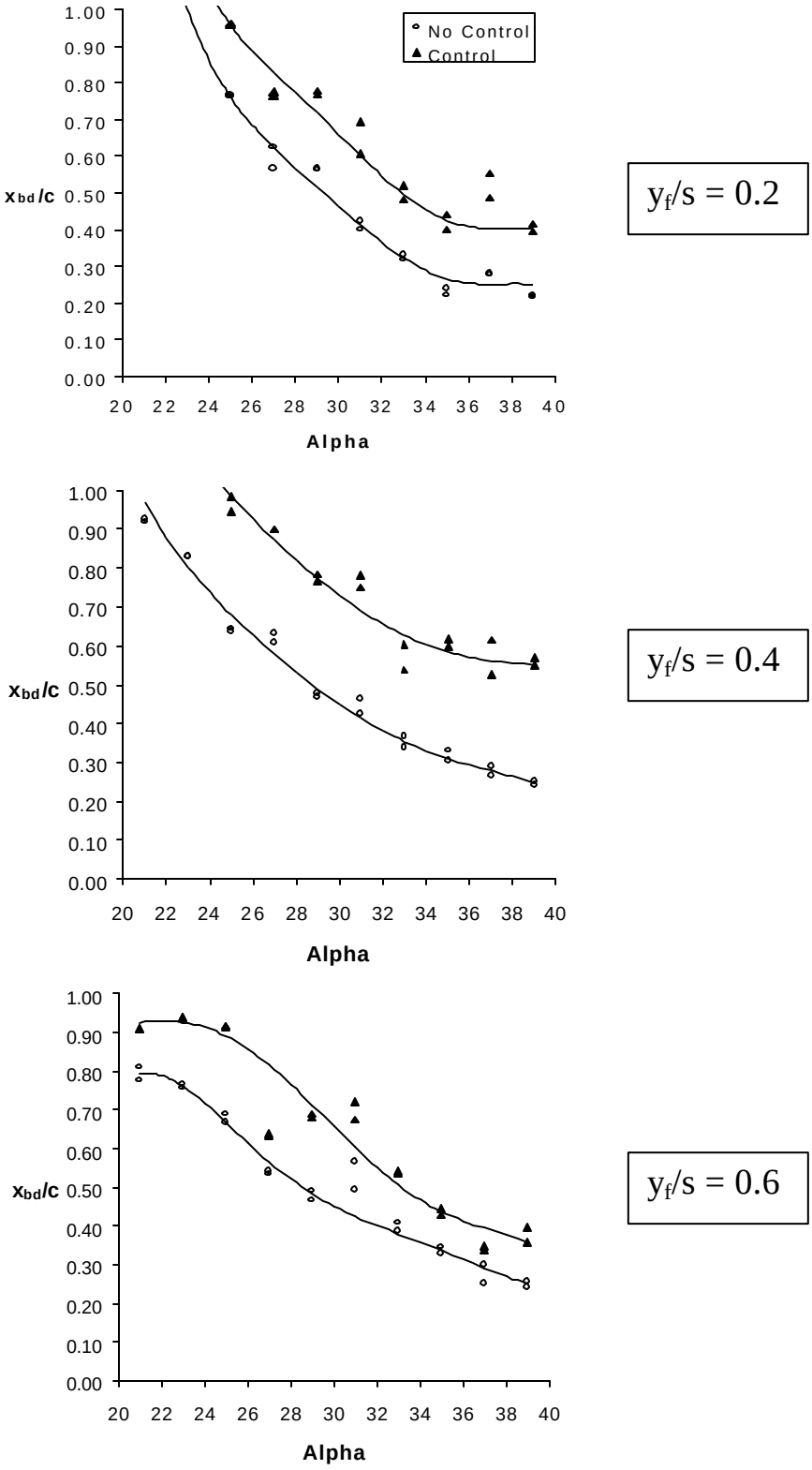


Figure 9: Variation of breakdown location with angle of attack for $\beta = 0°$.

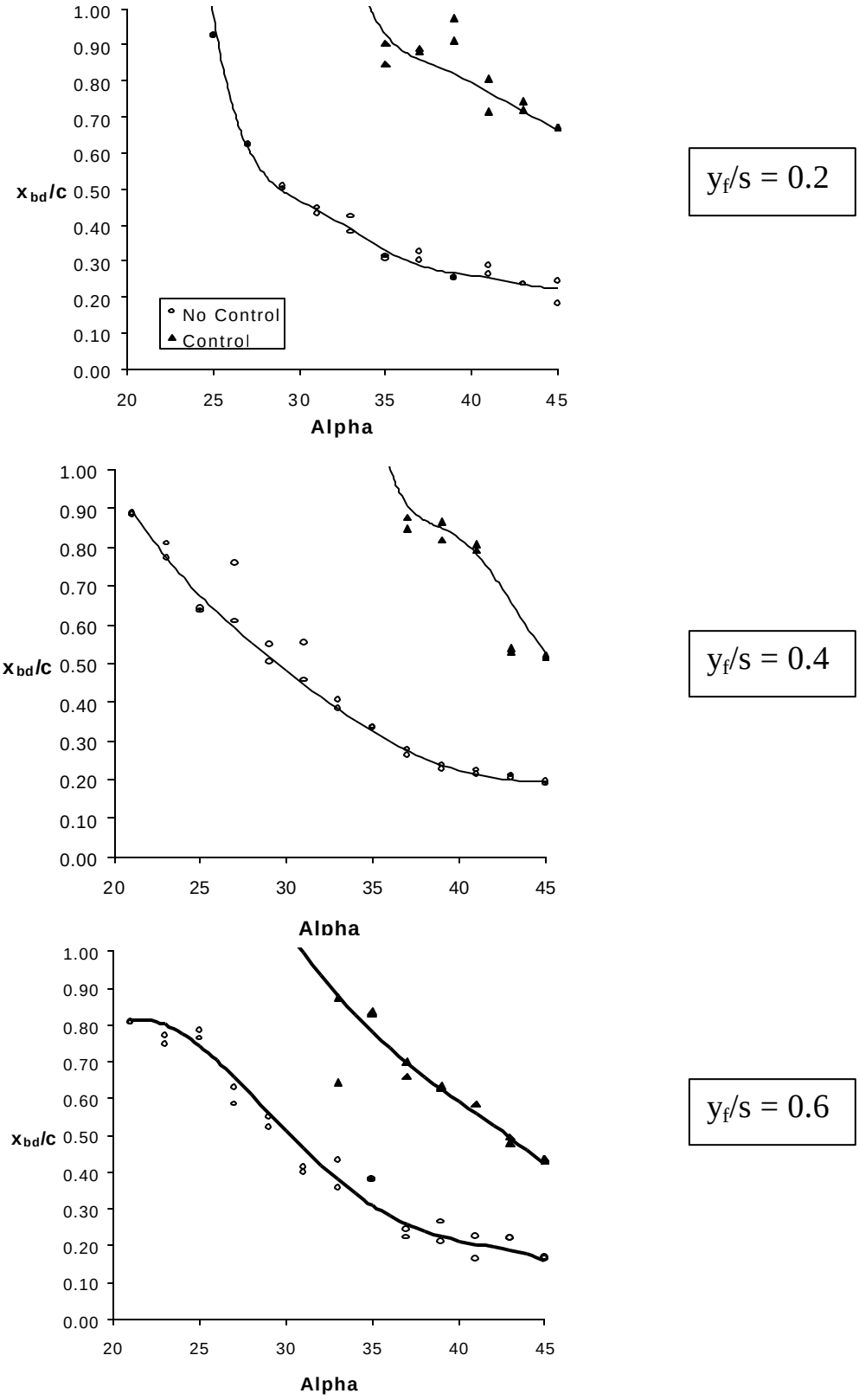


Figure 10: Variation of breakdown location with angle of attack for $\beta = 30°$.

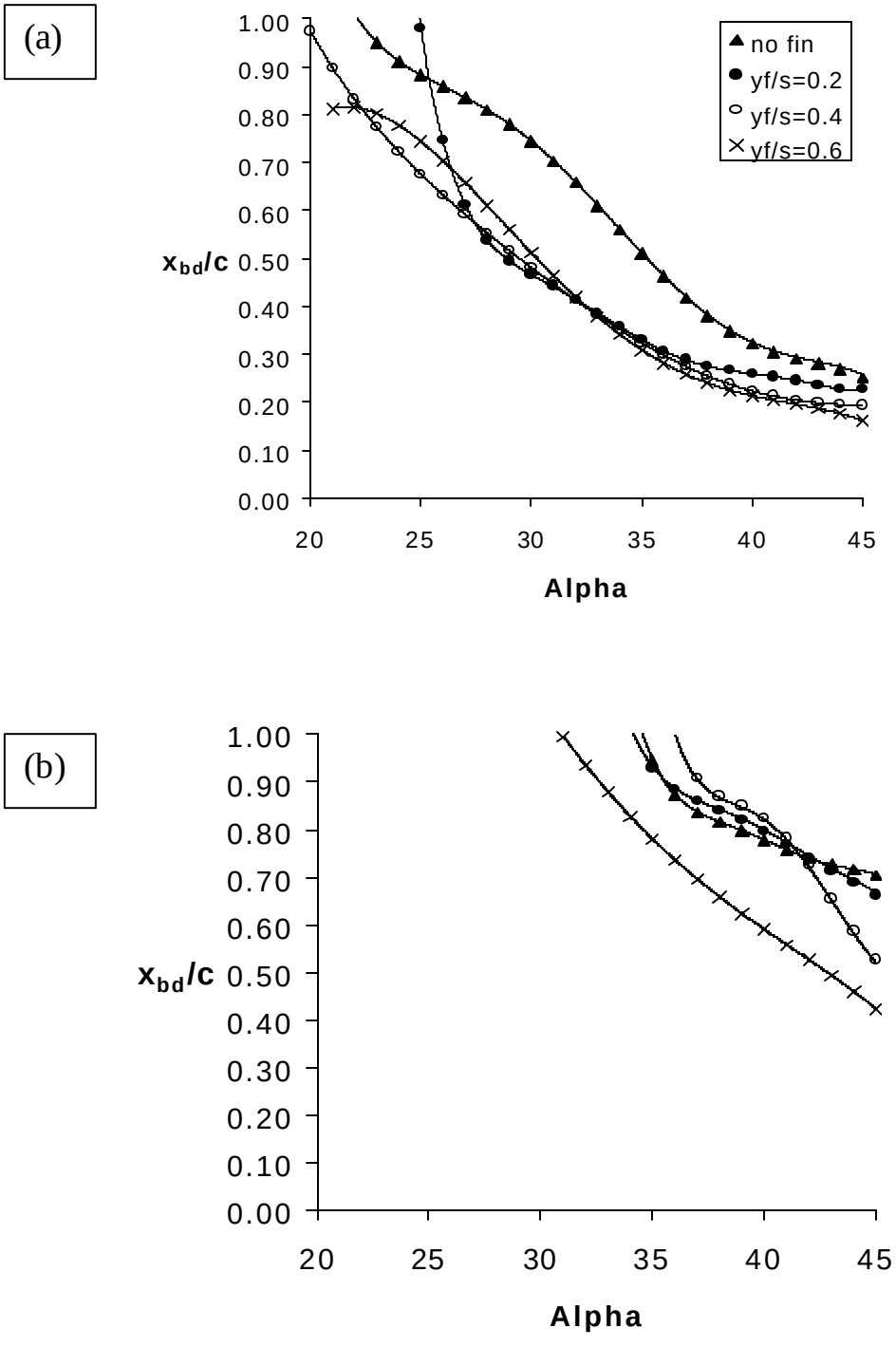


Figure 11: Variation of breakdown location with angle of attack for $\beta$=30° and (a) $U_{jet}/U_\infty = 0$, (b) $U_{jet}/U_\infty = 8.9$ ($C_\mu$=0.708).

(a)

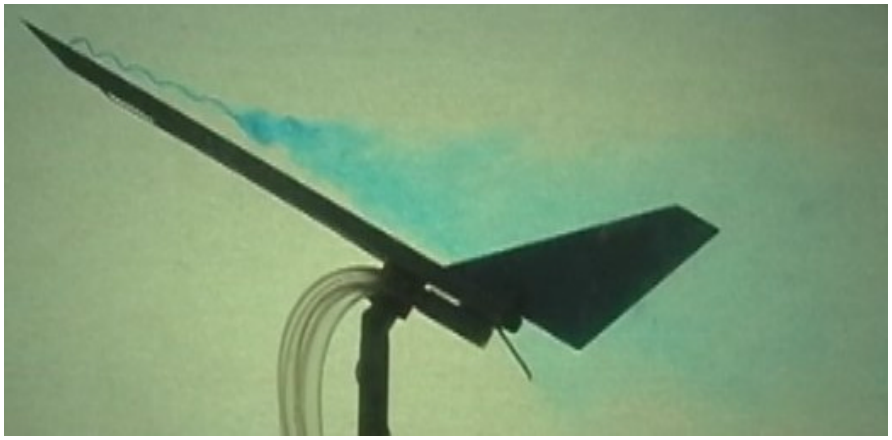

(b)

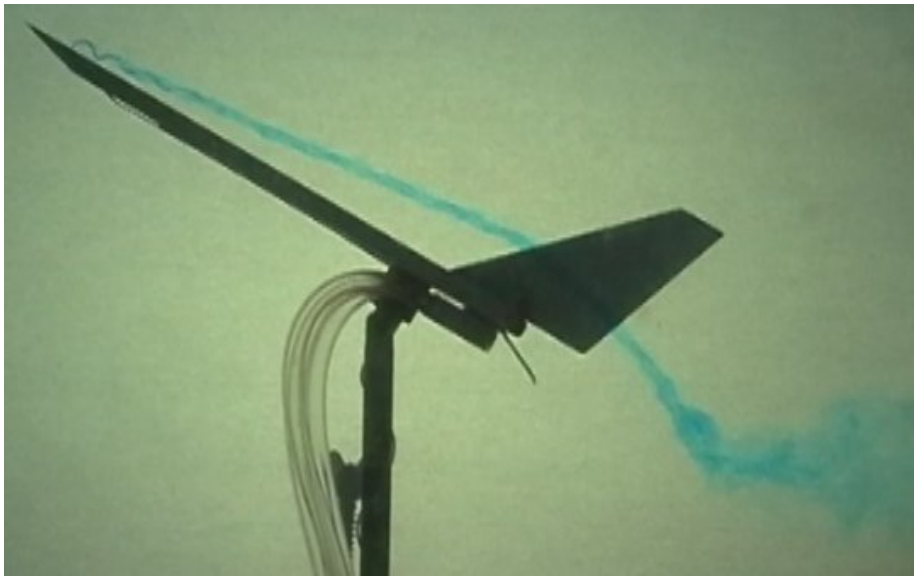

(c)

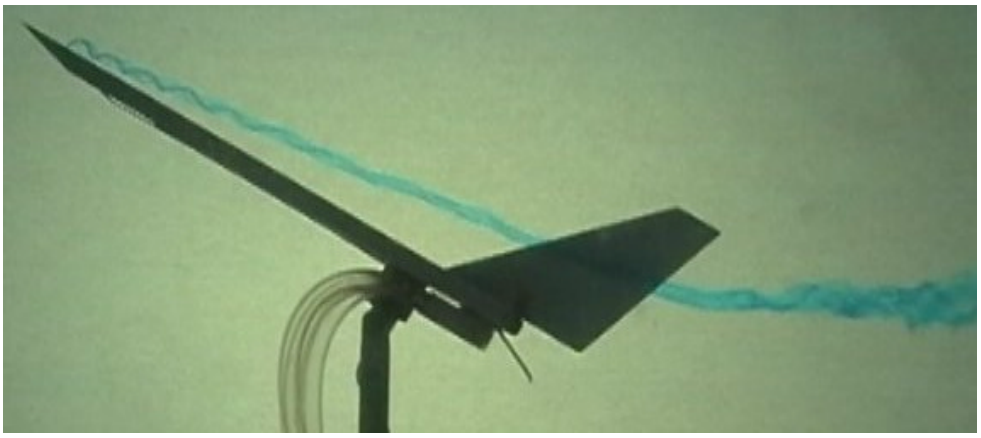

Figure 12: Flow visualization for (a) $U_{jet}/U_\infty = 0$, (b) $U_{jet}/U_\infty = 8.9$ ($C_\mu$=0.708), (c) right after the jet is turned off, $y_f/s$=0.2, $\alpha$=30°, $\beta$=30°.

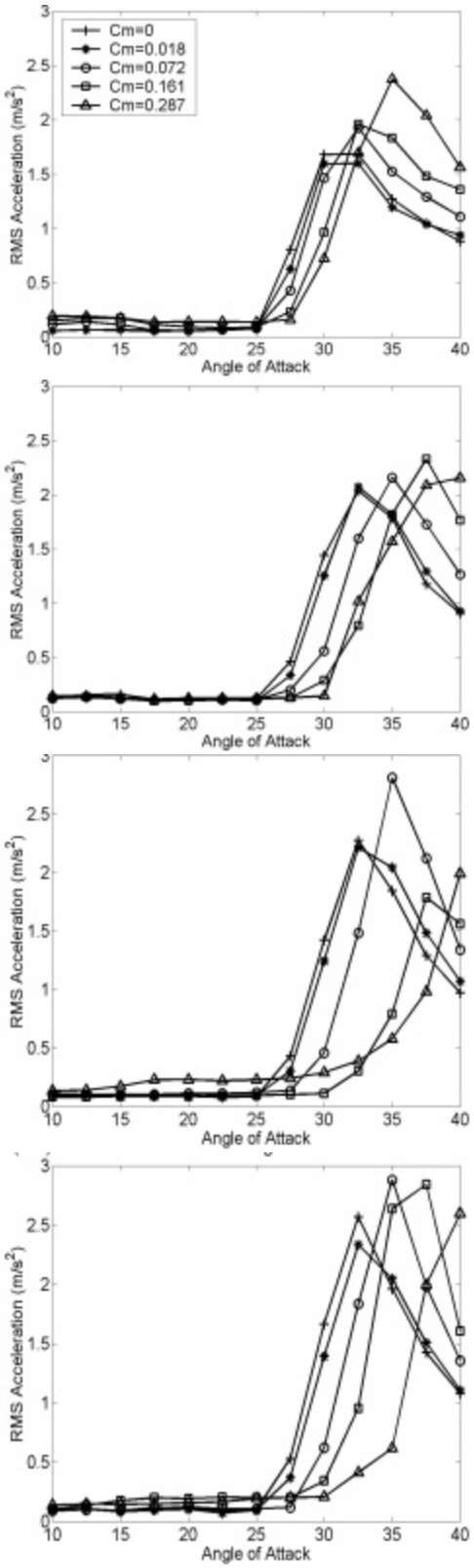


Figure 13: Variation of rms tip acceleration as a function of incidence for $y_f/s=0.2$.

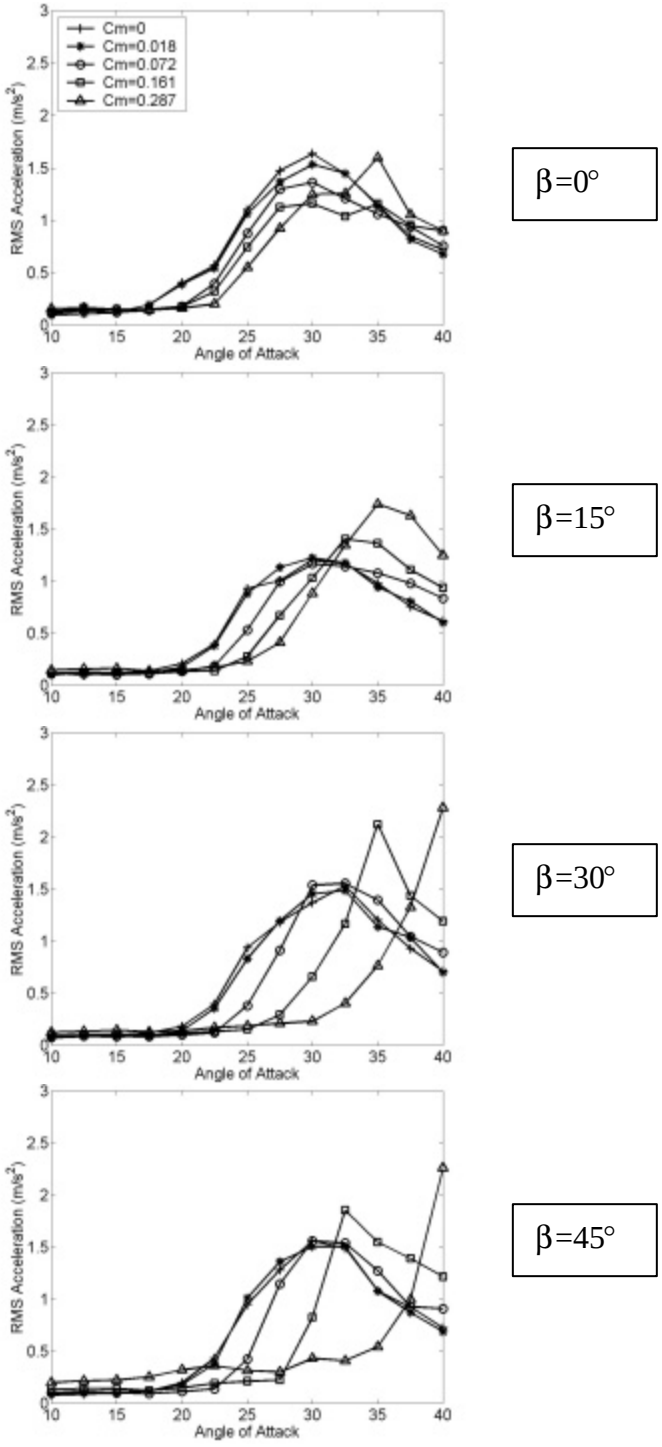


Figure 14: Variation of rms tip acceleration as a function of incidence for $y_f/s=0.4$.

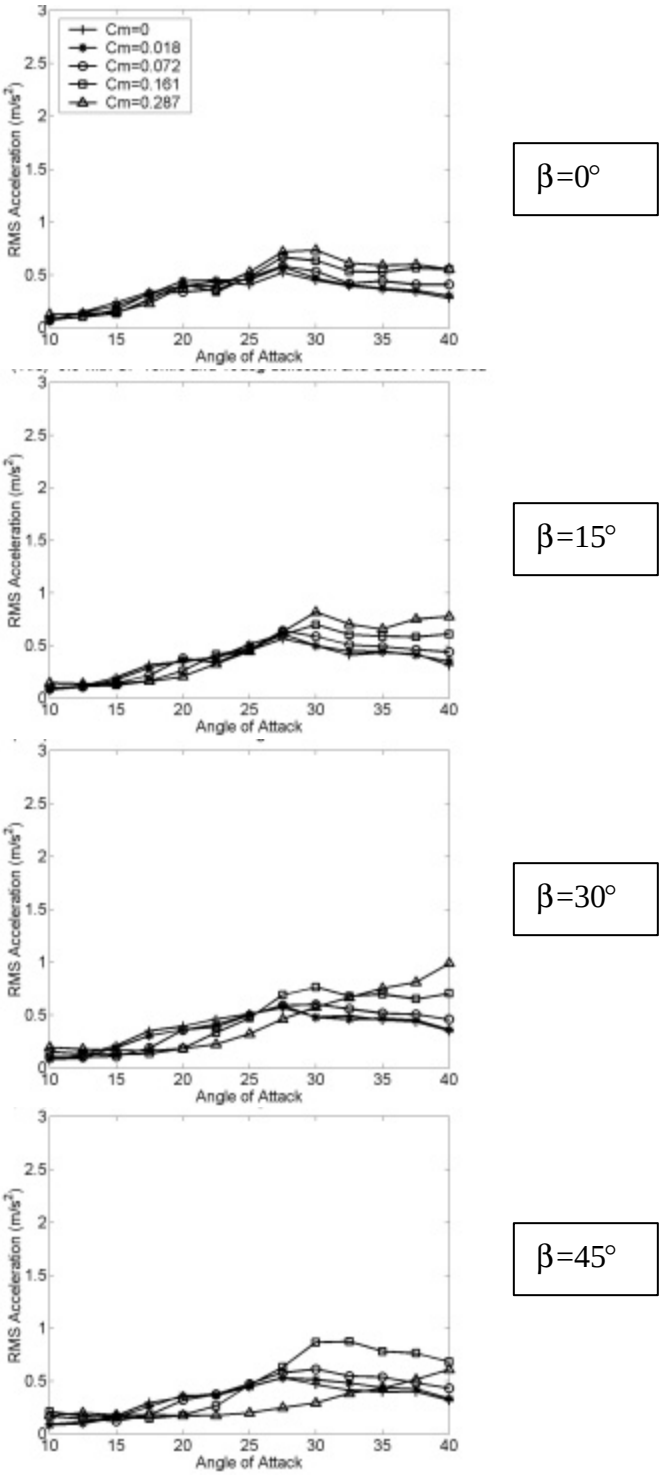


Figure 15: Variation of rms tip acceleration as a function of incidence for $y_f/s=0.6$.

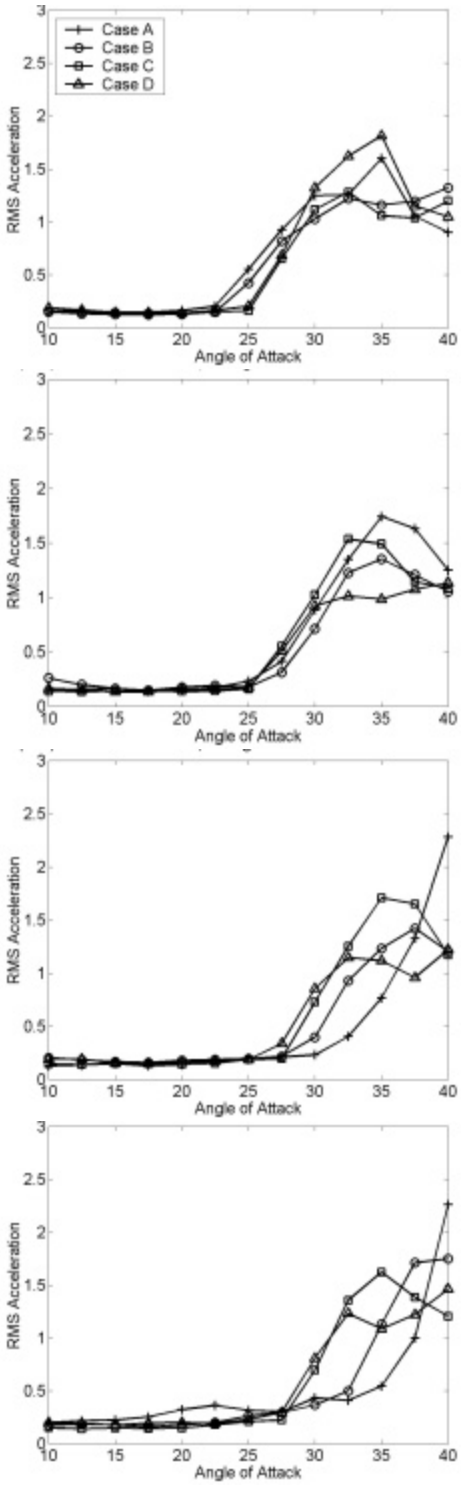


Figure 16: Variation of rms tip acceleration as a function of incidence for $y_f/s=0.4$ and $C_\mu=0.287$.